Hydrogen bonding in barbituric and 2-thiobarbituric acids: A theoretical and FT-IR study

ARTICLE *in* CHEMICAL PHYSICS · SEPTEMBER 2001

Impact Factor: 1.65 · DOI: 10.1016/S0301-0104(01)00440-2

4 AUTHORS, INCLUDING:

Lorenzo Gontrani
Sapienza University of Rome
56 PUBLICATIONS **872** CITATIONS
SEE PROFILE

Luigi Bencivenni
Sapienza University of Rome
110 PUBLICATIONS **1,316** CITATIONS
SEE PROFILE

ELSEVIER

Chemical Physics 271 (2001) 293–308

Chemical Physics

www.elsevier.com/locate/chemphys

Hydrogen bonding in barbituric and 2-thiobarbituric acids: a theoretical and FT-IR study

Fabio Ramondo [a,*], Andrea Pieretti [b], Lorenzo Gontrani [c,d], Luigi Bencivenni [e]

[a] *Dipartimento di Chimica, Ingegneria Chimica e Materiali, Università dell'Aquila, Loc Coppito, I-67100 L'Aquila, Italy*
[b] *Consorzio Applicazioni Supercalcolo Università e Ricerca (CASPUR), Università "La Sapienza", I-0085 Roma, Italy*
[c] *Dipartimento di Chimica e Chimica Industriale, Università di Pisa, I-56126 Pisa, Italy*
[d] *Tecnofarmaci S.C.p.A., I-00040 Pomezia (Roma), Italy*
[e] *Dipartimento di Chimica, Università "La Sapienza", I-00185 Roma, Italy*

Received 23 April 2001

Abstract

The effects of intermolecular hydrogen bonding on the molecular properties of barbituric acid (BA) and thiobarbituric acid are discussed on the basis of density functional theory calculations. B3LYP methods were applied to monomers and cyclic dimers. Trimer and hexamer of BA were studied as examples where several C=O and NH groups are involved in hydrogen bonding. The theoretical IR spectra of monomers and all oligomers here considered are compared with the FT-IR spectra measured in Ar and nitrogen matrices at different concentrations. © 2001 Elsevier Science B.V. All rights reserved.

1. Introduction

Barbituric acid (BA) (Fig. 1) is a widely studied molecular system which forms highly ordered structures through hydrogen bonding with substrates like 2,4,6-triaminopyrimidine, melamine and urea [1–4]. The molecular recognition process has been monitored by FT-IR [2,3] and UV/Vis [1,2,4], time of flight secondary ion mass [4] and photoelectron [4] spectroscopies. Notwithstanding FT-IR spectra in aqueous solution reveal that self-association of BA does not interfere with the formation of complex [2], dimerisation process of BA has been observed in concentrated and annealed matrix by FT-IR spectroscopy [5]. The intimate knowledge of tendency to self-associate of molecules is then an important point to consider when competitive processes of molecular aggregation are possible.

The identification of the structure of dimers and oligomers formed by self-association is however not straightforward and theoretical quantum mechanical methods successfully cooperate to provide much useful information on the structure, energy, properties and dynamics of molecular aggregates. Molecules of biological importance show several sites for hydrogen bonding interactions and the complexity of the intermolecular potential energy surface requires detailed studies of all the possible structures of dimers and oligomers [6]. Such structural problem has been recently investigated by some of us for uracil and thymine by combining theoretical and FT-IR spectroscopy studies [7]. A similar concerted theoretical and

* Corresponding author. Fax: +39-0862-433753.
E-mail address: ramondo@univaq.it (F. Ramondo).

0301-0104/01/$ - see front matter
PII: S0301-0104(01)00440-2

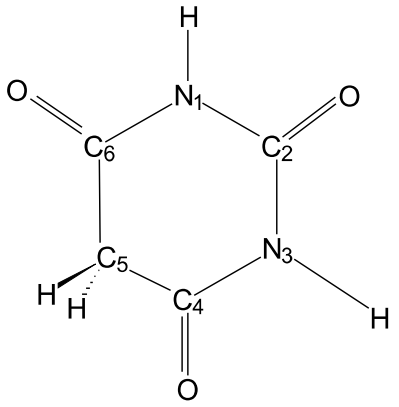

Fig. 1. Numbering of atoms in BA.

experimental approach may also be followed for BA where three C=O and two NH groups can be involved in several patterns of dimerisation. Previous studies [8–10] have shown that the density functional theory (DFT), combined with an appropriate basis set, reproduces important properties of hydrogen bonded molecules with accuracy comparable to that obtained with the more expensive conventional correlated methods, MPn.

The primary aim of the present work is therefore the study of some dimeric structures of BA in terms of energy, geometry and vibrational frequencies. Since no complete characterisation of the monomeric structure in gas phase has been yet reported, we have preliminarily undertaken a study on the isolated molecule through quantum mechanical methods. The FT-IR matrix spectrum, already measured in previous studies [5,11], has been then analysed on the basis of our computational results. The structural investigation on BA monomer has been completed with a parallel theoretical and experimental study on a sulphur analogous compound, 2-thiobarbituric. The spectral changes observed at high concentration matrix have been at last examined on the light of theoretical results obtained for some dimers and larger aggregates, such as a trimer and an hexamer, in the attempt to identify which structures are really formed during the aggregation process in matrix. The trimer and hexamer here studied offer the possibility to evaluate the effect of a progressive increase of number of hydrogen bonds on the molecular structure of BA. In addition, the hexamer is a suitable model simulating the neighbouring intermolecular interactions occurring in BA crystal.

2. Computational methods

Ab initio and DFT calculations were run on an Alpha AXP-3000/500 cluster of CASPUR at the University of Rome using the GAUSSIAN98 [12] package.

Geometry and vibrational frequencies of monomers were performed by analytical based gradient technique without any symmetry constraint. All the results were obtained using the DFT, employing the B3LYP (Becke's three parameter exchange [13] and Lee et al. correlation [14]) potentials, and the MP2 (f.c.) level of perturbation, combined with the 6-311++G(d,p) basis set [15].

The most stable tautomer of BA and the oxygen protonated species were further investigated in the framework of the G(MP2) theory [16] which yields final total energies which are effectively of MP2/6-311+G(3df,2p) quality. The protonation energies as well as the G2(MP2) calculated proton affinities (PA) were then calculated for two protonation sites of BA.

Dimers of BA and thiobarbituric acid (TBA) were investigated through six cyclic structures (Fig. 2) where two molecules interact by two C=O $\cdots$ H–N bonds (**2a**–**2d**), two C=S $\cdots$ HN (**2e**) bonds or a couple C=O $\cdots$ HN and C=S $\cdots$ HN of interactions (**2f**). No geometrical constraint was imposed to optimise geometry and calculate vibrational frequencies. However the localised stationary points correspond to structures slightly distorted from C_{2h} or C_s symmetry. All dimers were studied at the B3LYP/6-311++G(d,p) level. Furthermore, the topological properties of the hydrogen bond critical point were determined using the Bader's theory of atoms in molecules [17] using the subroutine implemented in GAUSSIAN98.

More extended aggregation processes were considered through the study of a trimer (Fig. 3) and an hexamer (Fig. 4) where the BA molecule forms four intermolecular hydrogen bonds. In the

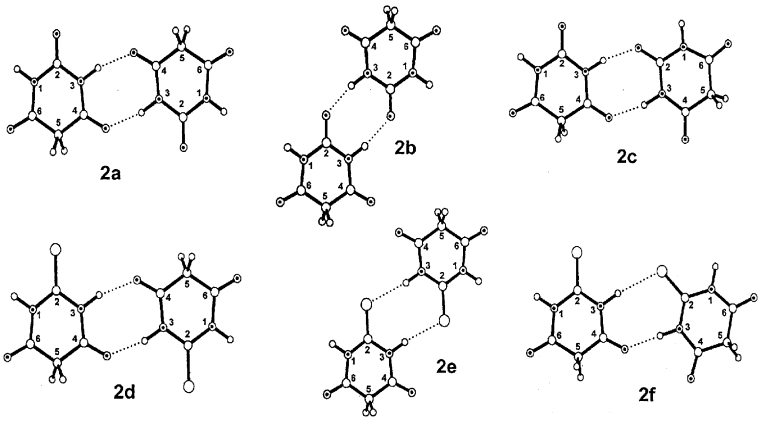

Fig. 2. Cyclic dimers of BA (**2a**, **2b** and **2c**) and TBA (**2d**, **2e** and **2f**). Oxygen and nitrogen atoms are marked by circles.

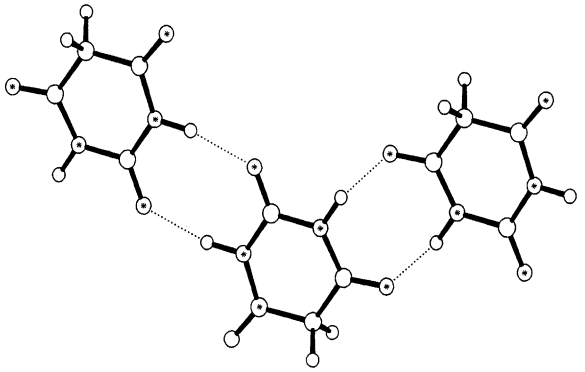

Fig. 3. BA trimer. Oxygen and nitrogen atoms are marked by stars.

trimer, the central molecule interacts with two other molecules forming a double closed structure involving the couple C2═O and HN1 with a second molecule and the couple C4═O and HN3 with the third molecule. The hexamer here proposed describes a different arrangement where a barbituric molecule connects simultaneously two molecules through two open hydrogen bonds (C4═O$\cdots$HN and N1H$\cdots$O═C) and a third molecule through a cyclic arrangement involving the couple C2═O and N3H. Geometry and frequencies of the trimer structure were studied at the B3LYP/6-311+G(d) level without any symmetry constraint whereas the hexamer was studied by imposing the C_{2h} symmetry. The correctness of the

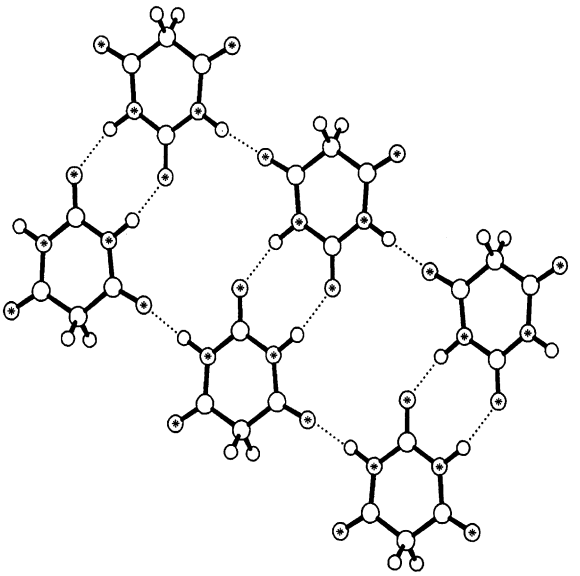

Fig. 4. BA hexamer. Oxygen and nitrogen atoms are marked by stars.

symmetry constraint is substantiated by the fact that the monomer, all cyclic dimers and the trimer show a symmetry plane, at least at the B3LYP/6-311++G(d,p) level of calculations. Because of the large size of the hexameric system, geometry optimisations and frequency calculations were carried out employing the ONIOM method [18] as implemented into the GAUSSIAN98 package. Using

this approach, the system was partitioned into two parts: the inner layer, that is the central dimer, was treated at the higher level of theory B3LYP/6-311+G(d) and the rest of the system was described by the computationally less demanding HF/6-31G(d) level. Since we are interested in the accurate description of the central region of the molecular system and in the homogeneous comparison with molecular parameters of dimers and trimer, the choice of B3LYP/6-311+G(d) level seems to be a reasonable compromise.

A test calculation was further carried out to assess the effects of the ONIOM approximation. The B3LYP/6-311+G(d) geometry of the trimer has been therefore compared with that of the same trimer obtained from the ONIOM method. In the latter case the system was partitioned in two parts: the dimer, treated at B3LYP/6-311+G(d) level whereas the third molecule was described at the HF/6-31G(d) level. The results undoubtedly show that the geometry of the region treated at the B3LYP/6-311+G(d) level is indeed very close to that obtained at full B3LYP/6-311+G(d) method with difference in bond lengths within one thousand of an Å.

3. Experimental

Commercial samples (Aldrich 98%) were purified by vacuum sublimation prior to the experiment and vapourised at ≈350 K from a glass oven located inside the vacuum chamber. The vapours coming from the molecular source were mixed with nitrogen or argon and deposited on a reflecting gold-plated copper cold-finger of a cryotip (202 CSA Air Products and Chemicals) at 12 K. Spectra were recorded by reflections using a Bruker IFS 113v inteferometer. 200 scans were accumulated at 1 cm^{-1} resolution. Different concentration matrices were obtained by regulating the temperature of vapourisation and the flow of the matrix gas. Cyclic annealing were repeated to encourage diffusion and association of monomer species. The FT-IR spectrum of a solid film of pure BA was also measured by deposition at 20 K. The deuterated compounds were prepared by exchange with D_2O at 350 K.

4. Results and discussion

4.1. Theoretical results

4.1.1. Barbituric acid and thiobarbituric acid tautomers

BA and its 2-sulphur derivative may exist in various tautomeric forms differing from each other by the position of the protons, which may be bound to either nitrogen and carbon atoms or oxygen (sulphur) atoms. Six tautomers are shown in Fig. 5 along with their relative energies calculated with respect to the most stable tautomer. All theoretical calculations report the trioxo tautomer for BA, henceforth indicated as BA, and the dioxo tautomer for TBA, indicated as TBA, to be the most stable tautomers. The high energy differences from the other tautomers suggest that gas phase of barbituric as well as 2-thiobarbituric acids consists of a single molecular species. This result is in agreement with a previous theoretical AM1 study [19] and with thermodynamic experimental data [20,21]. The trioxo tautomer of BA was found also in solid state from X-ray crystal structure determinations [22].

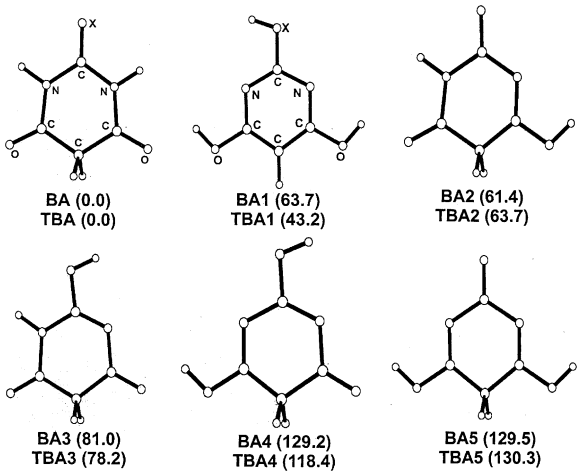

Fig. 5. Tautomers of barbituric, X=O (BA, BA1, BA2, BA3, BA5) and thiobarbituric, X=S (TBA, TBA1, TBA2, TBA3, TBA5) acids. MP2/6-311++G(d,p)//B3LYP/6-311++G(d,p) energy differences relative to the most stable BA and TBA tautomer are given in parentheses.

The order of stability found from our calculations for the gas-phase tautomers could be instead drastically altered in polar environments. This prevision is firstly suggested from the fact that some tautomers show several hydrogen bonding sites where the molecule may form specific and strong solute–solvent interactions. Secondly, the large differences in the values of dipole moment calculated for the various tautomers at all theoretical levels could affect the non-specific solute–solvent interactions, the latter ones strongly related to the magnitude of the dipole moment of solute. For example, the MP2/6-311++G(d,p) values of dipole moment for BA progressively increase from 0.379 D (BA) to 1.491 D (BA1), 2.944 D (BA2), 3.206 D (BA3), 3.525 D (BA4) and 4.608 D (BA5). Notwithstanding TBA and TBA1 have very close dipole moments (1.018 D and 0.908 D, respectively), a similar increase is expected for the remaining tautomers, 2.804 D (TBA2), 3.186 D (TBA3), 3.725 D (TBA4), 3.949 D (TBA5).

4.1.2. BA and TBA monomers

A preliminary study was therefore carried out on the most stable tautomers (BA) and (TBA) of the isolated molecules. The B3LYP method indicates that the ring in BA and TBA is planar and deviations from C_{2v} symmetry are indeed negligible for both the molecules. The ring is slightly distorted from planarity when MP2 levels are adopted with the methylene framework assuming a boat-shaped conformation (C_s symmetry). The C_{2v} structure corresponds to a first-order saddle point separating two equivalent energy minima of C_s symmetry and lies only about 1 kJ mol^{-1} higher in energy. Apart from such ring planarity deviations, bond lengths and valence bond angles have nearly equal values in the C_s and C_{2v} structures. Such a proximity in molecular geometries is fully reflected in the whole vibrational spectrum (frequencies and intensities) which slightly changes moving from the C_s and C_{2v} structures. In particular the A_2 modes, inactive in the infrared spectrum under C_{2v} symmetry, show negligible intensity in the lower C_s symmetry. Thus, infrared spectroscopy is not a suitable technique to investigate planarity of BA as well as TBA. Therefore to facilitate the description of the vibrational modes, henceforth the relative assignment will be discussed in terms of C_{2v} symmetry.

BA and TBA have 33 fundamentals modes which may be formally classified as six NH modes (stretching, in-plane and out-of-plane bending), six modes for the methylene group (two stretching, one scissoring, one wagging, one twisting and one rocking), 12 ring modes (six stretching, three in-plane bending and three torsion) and nine C=O modes for BA or six C=O and three C=S modes for TBA (stretching, in-plane and out-of-plane bending). Table 1 shows the unscaled harmonic vibrational frequencies, obtained at the B3LYP/6-311++G(d,p) and MP2/6-311++G(d,p) levels. The effects of a further extension of the basis set were evaluated through geometry optimisations and frequency calculations on BA at the B3LYP/6-311++G(3df,2pd) level; however the values are virtually the same ones obtained at the lower B3LYP/6-311++G(d,p) level. A direct comparison between normal modes of the two molecules indicates that substitution of oxygen with sulphur produces small differences in the vibrational spectrum. Outstanding changes are limited to the C=O stretching region, where the highest frequency mode of BA obviously disappears in TBA and is found as C=S stretching at 1146 cm^{-1}, and to the NH bending and CN stretching regions. In particular, the ω_8 and ω_{10} modes shift at higher frequency whereas the ω_{11} and ω_{12} modes undergo small down-field shifts. Since all these modes involve CN stretching strongly mixed with NH bending vibrations, such a comparison suggests that sulphur substitution produces a variation of π-conjugation in the CN bonds. The smaller π-character of the C=S with respect to C=O bond discourages delocalisation of electrons in the framework S=C–N increasing consequently the CN bond order. Consistently with this hypothesis is the fact that the C2N1 bond shortens by about 0.014 Å in TBA whereas the N3C4 bond remains practically unchanged (0.004 Å) in both the molecules. The larger rotation barrier about the CN bond of thioformamide with respect to formamide determined from ab initio studies [23] supports our results for BA and TBA. A convincing proof of the increased π-character of the CN bond of TBA is found in the stiffening of the out-of-plane NH

Table 1
Vibrational frequencies (cm^{-1}) and IR band intensities ($km\,mol^{-1}$), in parentheses, of BA and TBA

No	Major internal coordinates[a]	Symmetry[b]	B3LYP/6-311++G(d,p)		MP2/6-311++G(d,p)	
			BA[c]	TBA	BA	TBA
ω_1	νNH	A_1	3591 (49)	3587 (31)	3615 (53)	3606 (29)
ω_2	νNH	B_2	3589 (111)	3583 (110)	3614 (113)	3604 (115)
ω_3	νCH_2	B_2	3098 (1)	3096 (1)	3188 (7)	3186 (7)
ω_4	νCH_2	A_1	3066 (2)	3064 (1)	3088 (6)	3085 (3)
ω_5	νC2═O/νC═S[d]	A_1	1820 (78)	1146 (199)	1832 (537)	1198 (227)
ω_6	νC4═O + νC6═O[d]	A_1	1800 (892)	1805 (378)	1809 (414)	1801 (402)
ω_7	νC4═O + νC6═O[d]	B_2	1784 (604)	1783 (656)	1790 (477)	1784 (519)
ω_8	δNH + νCN + δCH_2	A_1	1452 (49)	1542 (530)	1456 (66)	1560 (737)
ω_9	δCH_2	A_1	1417 (18)	1423 (4)	1439 (79)	1444 (13)
ω_{10}	δNH + νCN + δCH_2	B_2	1416 (176)	1425 (182)	1433 (310)	1434 (217)
ω_{11}	νCN	B_2	1404 (136)	1381 (46)	1409 (8)	1385 (17)
ω_{12}	νCN	A_1	1342 (373)	1334 (588)	1362 (308)	1361 (556)
ω_{13}	CH_2 wagging	B_2	1310 (8)	1312 (9)	1310 (16)	1311 (15)
ω_{14}	νCN + νCC	B_2	1220 (141)	1225 (102)	1257 (91)	1262 (64)
ω_{15}	CH_2 twisting	B_2	1219 (2)	1217 (>0)	1200 (31)	1198 (28)
ω_{16}	νCN + νCC	A_1	1019 (11)	1024 (>0)	1028 (2)	1025 (6)
ω_{17}	CH_2 rocking	B_1	953 (9)	951 (10)	976 (11)	971 (15)
ω_{18}	νCC + νCN	A_1	919 (2)	885 (2)	942 (2)	919 (9)
ω_{19}	νCC + νCN	B_2	914 (0)	898 (8)	934 (>0)	920 (5)
ω_{20}	γC2═O/γC2═S	B_1	752 (55)	617 (3)	755 (64)	615 (>0)
ω_{21}	γNH	B_1	687 (174)	708 (159)	693 (144)	713 (150)
ω_{22}	γNH	A_2	681 (0)	688 (0)	676 (12)	678 (13)
ω_{23}	δ ring	A_1	631 (1)	554 (>0)	640 (1)	577 (2)
ω_{24}	δC═O	B_2	623 (9)	588 (2)	620 (15)	596 (9)
ω_{25}	γC4═O + γC6═O	A_2	588 (0)	590 (0)	588 (8)	585 (3)
ω_{26}	δ ring	B_2	488 (14)	492 (17)	479 (4)	505 (6)
ω_{27}	δ ring	A_1	482 (41)	446 (53)	451 (27)	436 (40)
ω_{28}	γC4═O + γC6═O	B_1	477 (>0)	478 (>0)	540 (15)	478 (7)
ω_{29}	δC═O	A_1	383 (16)	368 (5)	391 (13)	375 (5)
ω_{30}	δC═O/δC═S	B_2	382 (35)	256 (11)	381 (31)	262 (10)
ω_{31}	τ ring	B_1	135 (>0)	124 (>0)	139 (4)	124 (>0)
ω_{32}	τ ring	A_2	116 (0)	112 (0)	118 (>0)	116 (5)
ω_{33}	τ ring	B_1	10 (11)	19 (12)	92 (6)	87 (4)

[a] ν: stretching, δ: in-plane bending, γ: out-of-plane deformation, τ: torsion.
[b] Under C_{2v} symmetry.
[c] The B3LYP/6-311++G(3df,2pd) frequencies of the A_1 and B_2 modes differ from the B3LYP/6-311++G(d,p) values within a maximum of five wave numbers; the A_2 and B_1 modes show instead higher frequencies, namely ω_{20} (768 cm^{-1}), ω_{21} (699 cm^{-1}), ω_{22} (698 cm^{-1}), ω_{25} (595 cm^{-1}), ω_{28} (482 cm^{-1}), ω_{31} (143 cm^{-1}), ω_{32} (122 cm^{-1}), ω_{33} (35 cm^{-1}).
[d] Description at the MP2 level.

vibrations which increase in frequency by about 20 cm^{-1} in the sulphur containing compound. Apart from such variations in the C2N1 bond distance, a quick inspection of the geometry of the ring, bond lengths and bond angles, reveals that the sulphur substitution does not alter significantly the ring structure.

The examination of the vibrational frequencies reveals further important structural features: BA has two NH groups equivalent whereas the C═O groups show different chemical properties. The G2(MP2) values of proton affinity indicate that basicity of C2═O groups (PA = 782 $kJ\,mol^{-1}$) is higher than C4═O (PA = 775 $kJ\,mol^{-1}$). Notwithstanding basicity gap is very small, only 7 $kJ\,mol^{-1}$, such important chemical property is well reflected in their characteristic vibrations. The higher frequency vibrations, ω_5 and ω_6, involve in

fact the more basic C2=O group whereas the lowest frequency mode is a B_2 symmetry vibration localised mainly on the less basic C4=O and C6=O groups. This fact emerges also from the C=O out-of-plane bending vibrations, ω_{20}, ω_{25} and ω_{28} (752, 588 and 477 cm^{-1}) modes where the highest frequency mode exclusively involves the C2=O group. On the other hand, the equivalence of the NH groups is well witnessed in those modes largely localised on such groups such as stretching (3591, 3589 cm^{-1}) and out-of-plane bending, (687 and 681 cm^{-1}) where symmetric and asymmetric vibrations have very close frequencies. The NH in-plane bending modes are instead strongly mixed with stretching vibrations of the ring bonds and this is the main reason of the outstanding differences between symmetric (A_1) and asymmetric (B_2) vibrations of the each normal mode.

As a matter of fact normal mode analysis of the three C=O stretching modes show discrepancies when B3LYP and MP2 results are compared. Mixing between the C2=O and C4=O or C6=O stretching coordinates is negligible at the MP2 level and it is easy identify the highest frequency mode as an isolated C2=O stretching and the remaining modes as a symmetric, ω_6, and asymmetric, ω_7, vibration of the C4=O and C6=O groups. On the contrary, the B3LYP predicts a strong mixing between the C2=O stretching coordinate and the symmetric vibration of the C4=O and C6=O groups in both the ω_5 and ω_6 modes. The different composition of C=O stretching modes plays an important role in the intensities of the three modes. All three bands ω_5, ω_6 and ω_7 show strong intensities at the MP2 level, in a substantial agreement with the experiment [5], whereas the ω_5 band is clearly much weaker than ω_6 and ω_7 absorptions at the B3LYP. The different agreement with the measured IR spectrum could be a valid support to the fact that MP2 gives a more accurate description of the C=O stretching modes with respect to B3LYP.

4.1.3. Hydrogen bonded BA and TBA: dimers, a trimer and an hexamer

Three cyclic dimers were here considered for BA: two centrosymmetric structures where hydrogen bond involves C4=O (**2a**) or C2=O (**2b**) and a third one (**2c**) where both C4=O···HN and C2=O···HN hydrogen bonds are formed. TBA can form only one centrosymmetric dimer through C=O···HN (**2d**), whereas further cyclic dimers can be formed by involving C=O···HN and C=S···HN (**2e**) or two C=S···HN (**2f**) hydrogen bonds. Notwithstanding no basis set superposition error corrections were accomplished since the main scope of the present work is not the accurate investigation of the stability of the complexes, our B3LYP/6-311++G(d,p) calculations suggest that the three dimers of BA show stability indeed similar with a slight preference for **2a** structure. This is largely expected on the basis of previous studies on uracil and derivatives where it emerged that hydrogen bonding (energy and structural deformations) is largely governed by the acidity of the NH groups more than basicity of C=O groups [7]. Since BA has equivalent NH groups, it can form dimers with stability indeed very similar. TBA dimers show instead a preference for a double C=O···HN interaction (**2d**) with respect to the alternative dimers, less stable by 7 $kJ\,mol^{-1}$ (**2e**) and 15 $kJ\,mol^{-1}$ (**2f**).

The distortions of the molecular geometry caused by dimerisation are those predicted for hydrogen bonded amides [24], namely lengthening of C=O and NH bonds and simultaneous shortening of the CN bond. They reveal changes in the π-character of the amide group and suggest that the contribution of the polar canonical form $^{+}N{=}C{-}O^{-}$ as a resonance structure of BA increases for hydrogen bonded molecules. A detailed analysis of the values of bond lengths for the dimers of BA and TBA, reported in Table 2, suggests that those dimerisation processes occurring through the formation of different hydrogen bonds (**2c** or **2f**), produce molecules with geometries as arising from the superposition of separate, nearly independent effects of each hydrogen bonding interaction. This is the case of the **2c** dimer, the structure of which is obtained by adding the deformations produced in the **2a** and **2b** dimerisation processes or **2f** dimer obtained by adding the effects of the single **2d** and **2e** dimerisations.

The cooperativity effect was also examined from the changes in the intermolecular hydrogen bonds distances. The values O···N distances (see

Table 2
B3LYP/6-311++G(d,p) selected bond distances (Å) of BA and TBA monomers, $(BA)_2$ and $(TBA)_2$ dimers, $(BA)_3$ trimer and $(BA)_6$ hexamer and topological electron density properties of the bond critical points in the intermolecular hydrogen bond

	BA	$(BA)_2$			$(BA)_3$[a,b]	$(BA)_6$[a,c]	TBA	$(TBA)_2$		
		C2═O···HN3 C2═O···HN3	C4═O···HN3 C4═O···HN3	C2═O···HN3 C4═O···HN3				C4═O···HN3 C4═O···HN3	C═S···HN3 C═S···HN3	C4═O···HN C═S···HN3
C2N3	1.392	1.378	1.395	1.378/1.395	1.390	1.392	1.378	1.382	1.368	1.381/1.367
N3C4	1.389	1.392	1.373	1.392/1.373	1.375	1.371	1.393	1.378	1.397	1.377/1.397
C4C5	1.516	1.518	1.513	1.518/1.513	1.511	1.513	1.514	1.511	1.515	1.511/1.515
C5C6	1.516	1.514	1.515	1.514/1.515	1.517	1.518	1.514	1.513	1.512	1.513/1.511
C6N1	1.389	1.391	1.387	1.391/1.387	1.389	1.384	1.393	1.390	1.394	1.392/1.393
N1C2	1.392	1.387	1.394	1.387/1.394	1.381	1.377	1.378	1.381	1.377	1.380/1.370
C2═X	1.207	1.220	1.206	1.220/1.206	1.217	1.219	1.652		1.664	1.649/1.667
C4═O	1.208	1.208	1.220	1.208/1.220	1.219	1.217	1.208	1.219	1.207	1.219/1.207
C6═O	1.208	1.207	1.209	1.207/1.209	1.208	1.210	1.208	1.208	1.208	1.208/1.208
N3H	1.013	1.027	1.028	1.028/1.028	1.024	1.029	1.013	1.027	1.026	1.026/1.028
N1H	1.013	1.013	1.013	1.013/1.013	1.026	1.029	1.013	1.013	1.013	1.013/1.013
O···N		2.906	2.904	2.905/2.901	2.929 2.922 2.937 2.940	2.865		2.910		2.906
S···N									3.459	3.450
ρ(H···O)[d]		0.0268	0.0273	0.0272/0.0274				0.0264		0.0275
ρ(H···S)[d]									0.0161	0.0179
$\nabla^2\rho$[e]		0.0989	0.0987	0.0998/0.0990				0.0974	0.0400	0.1012–0.0419

[a] B3LYP/6-311+G(d) values.
[b] Bond distances relative to the central molecule.
[c] Bond distances relative to the couple of central molecules.
[d] Electron density (atomic units).
[e] Laplacian of electron density (atomic units).

Table 2) are very similar in all three cases and therefore they are only marginally affected by the dimerisation pattern. Very small are also the variations in the N···S intermolecular bond distances which suggest the presence of a slight cooperative effect in the TBA **2f** dimer where both the C=S···HN and C=O···HN interactions are present.

Further insight into the cooperativity in hydrogen bonding interactions is afforded by inspection of the topological electron density properties. In all the dimers the intermolecular hydrogen bond was characterised by the presence of bond critical point between the hydrogen atom and the acceptor oxygen or sulphur atom. It has been shown [17] that for hydrogen bonding interactions the electron density, ρ, at the bond critical point is low and its curvature (determined from the Laplacian of the electron density, $\nabla^2\rho$) is positive. These conditions are fulfiled in the bond critical points for all the dimers, as shown in Table 2. The values of ρ and $\nabla^2\rho$ calculated for BA dimers are indeed similar whereas only small changes are calculated for TBA dimers. Such topological properties are indicative of a negligible cooperativity effect of the two hydrogen bonding interaction, at least for the couple of C=O···HN bonds.

The vibrational spectrum of each dimer consists of 72 normal modes and most of the intramolecular modes of the isolated molecule are easily recognisable in dimer. It is therefore easy to evaluate the shifts experienced by these modes upon dimerisation (see Table 3). From a careful insight of their values the following comments can be made.

Self-association through hydrogen bonding causes well known changes in the frequency values; that is red-shifts for the C=O and NH stretching modes, large blue-shifts for the out-of-plane NH bending frequencies and moderate blue-shifts for all modes involving in-plane NH bending and ring bond stretching.

Some modes show a pattern of frequency shifts sensitive to the type of dimerisation process. This is the case of those modes where the CN stretching vibrations are dominant, such as the ω_{11}, ω_{12}, ω_{14} and ω_{16} ones. As concerning the C=O stretching modes, higher shifts are predicted for the B_2 vibration whereas the highest frequency mode, ω_5, seems to be unaffected by intermolecular association. On the other hand, other vibrations suffer shifts which are not typical of the dimer structure, for example the B_2 modes of the νNH and γNH vibrations as well as the ω_8 and ω_{10} modes, vibrations with NH in-plane and CN stretching contributions.

Consistently with the geometrical deformations, frequency shifts experienced by normal modes of each monomer in the **2c** dimer, where different hydrogen bonding interactions coexist, are simply a superposition of those calculated for each interaction from the centrosymmetrical dimers. Therefore also the frequency shifts suggest the absence of mutual influence between the C2=O···HN and C4=O···HN interactions as a consequence of the nearly equivalence of the two hydrogen bonds. In contrast with this case, cooperativity plays an important role in those cyclic dimerisation processes where the sites of intermolecular interaction shows different acid/basic properties, as found for uracil [7].

A model where two C=O and two NH groups form simultaneously hydrogen bonding is the hexamer of BA shown in Fig. 4. Such a complex can be formally considered as the dimer **2b** having additional interactions involving the C4=O group and the remaining NH group. As for the hexamer here studied, BA crystal contains molecules bonded through a couple of C2=O···HN bonds, a couple of C4=O···HN bonds whereas the third C=O position is not involved in hydrogen bonding [22]. The geometry of the couple of molecules localised in the central zone of hexamer, when compared with that of the corresponding isolated dimer, shows significant differences. As already described for dimers, the pattern of shortening and lengthening of the CN bond distances, deriving from an increases of the π-character of the CN bonds, reveals the importance of polar canonical forms for hydrogen bonded species. In the case of the hexamer, we observe a simultaneous shortening of two CN bonds, namely C4N3 and C2N1. This suggests that the structure with a double $^{+}$N=C–O^{-} character becomes the main polar canonical form when BA is involved in four hydrogen bonds.

Table 3
B3LYP/6-311++G(d,p) selected frequencies (cm^{-1}) of BA monomer, $(BA)_2$ dimers, $(BA)_3$ trimer and $(BA)_6$ hexamer and comparison values measured in concentrated Ar matrix and solid film

		BA	$(BA)_2$				$(BA)_3$[a]	$(BA)_6$[b]		Matrix	Solid film
			C2=O···HN3 C2=O···HN3	C4=O···HN3 C4=O···HN3	C2=O···HN3 C4=O···HN3			A_u	A_g		
ω_1	νNH	3591	3589	3589	3589	3589	3411–3388	3386	3383	3230	3210
ω_2	νNH	3589	3349	3364	3352	3352	3384–3359	3331	3309		
ω_5	3νC=O sym	1820	1820	1816	1820	1814	1807	1803	1798		1749
ω_6	3νC=O asym	1800	1798	1788	1797	1788	1780	1779	1783		1726
ω_7	νC4=O + νC6=O	1784	1756	1771	1751	1769	1760	1754	1760	1734	1700
ω_8	δNH + νCN	1452	1488	1481	1489	1484	1495	1506	1501	1459	1460
ω_{10}	δNH + νCN	1416	1437	1440	1437	1440	1486	1486	1487	1445	1434
ω_{11}	νCN	1404	1403	1430	1405	1431	1440–1437	1438	1440		
ω_{12}	νCN	1342	1371	1342	1368	1341	1377–1368	1377	1371	1360	1384
ω_{14}	νCN + νCC	1220	1240	1221	1239	1222	1247	1249	1251	1233	1251
ω_{16}	νCN + νCC	1019	1026	1040	1023	1042	1047	1048	1049	1030	1038
ω_{18}	νCC + νCN	919	928	923	929	921	933	933	929		
ω_{19}	νCC + νCN	914	921	916	916	919	925	926	924		
ω_{20}	γC2=O	752	751	752	751	753	755	756	754		
ω_{21}	γNH	687	889	873	890	857	916	946	927	860–830	800
ω_{22}	γNH	681	686	684	688	688	876–861	911	899		
ω_{23}	δ ring	631	636	635	641	635	639	652	658		
ω_{24}	δC=O	623	631	633	630	633	636	632	629		
ω_{25}	γC4=O + γC6=O	588	608	609	610	612	628	629	628		
ω_{26}	δ ring	488	494	492	492	494	498	509	513		
ω_{27}	δ ring	482	490	487	489	485	495	494	492		
ω_{28}	γC4=O + γC6=O	477	480	480	482	481	487	483	483		
ω_{29}	δC=O	383	408	407	408	395	413	418	403		
ω_{30}	δC=O	382	382	383	386	383	393	376	378		

[a] Frequencies of modes mainly localised on the central molecule.
[b] Frequencies of A_u and A_g modes mainly localised on the couple of central molecules.

As for molecular geometry, also vibrational frequencies of the hexamer allow to evaluate the variations of the vibrational spectrum that occur increasing progressively the complexity of hydrogen bonding coordination. In addition, the hexamer spectrum may be a valuable approach to estimate the vibrational spectrum predicted for a molecule in the BA crystal. Significant information can be obtained by an homogeneous comparison between the frequencies of the A_u and A_g modes localised on the two central molecules of hexamer, the frequencies of the monomer and those of the **2b** dimer, as reported in Table 3. In contrast with a simple dimerisation, all modes of groups of the central molecules in hexamer involved in hydrogen bonding suffer frequency shifts. For example, all the three C=O stretching vibrations are red-shifted, whereas all the modes involving NH in plane bending and CN stretching are significantly blue-shifted. In addition, the amount of each frequency change is higher by increasing the number of hydrogen bonds. All this indicates that the involvement of a second C=O and NH group in additional hydrogen bonds has a synergic effect on the strength of the double central C2=O···HN interaction.

When the same investigation was carried out for the trimer, and in particular for the central molecule, we found a molecular geometry (Table 2), as well as vibrational frequencies (Table 3), indeed very close to those calculated of the hexamer. Such a comparison lead to predict that when BA self-associates by involving four groups, namely two C=O and two NH, it forms oligomers having molecular structures and in particular vibrational frequencies virtually indistinguishable.

4.2. Comparison with matrix FT-IR spectra

4.2.1. Dilute matrix IR spectra

The B3LYP vibrational frequencies of BA are compared in Table 4 with the experimental values measured in argon matrix for BA, *N*,*N*′-dideuterated, $BA(D_2)$, (see Fig. 6) and fully deuterated, $BA(D_4)$ [5], isotopomers. Such a comparison reveals that the stretching modes, νNH (ND) and νC=O, as well as the NH out-of-plane bending vibrations, γNH, are reproduced with scaling factors ranging from 0.93 to 0.99. The near degeneracy predicted in the νNH and γNH modes explains the presence in the matrix spectra of single bands in the νNH, νND and γNH regions. A similar degeneracy was observed also for the symmetric and asymmetric vibrations of NH in-plane bending, δNH, which were previously assigned to the bands at 1322 and 1319 cm^{-1} [5]. The ring bond stretching modes were identified with the absorptions at 1433, 1418, 1222, 1192 cm^{-1} (CN stretching) and 1010, 939 cm^{-1} (CC stretching) [5]. There is a general agreement with the calculated frequencies, however discrepancies are found for the δNH modes. Such vibrations have large contributes into the modes ω_8 and ω_{10}, where they are indeed dominant, and in all the modes involving ring bond stretching, such as the CN (ω_{11}, ω_{12}, ω_{14} and ω_{16}) and CC stretching modes (ω_{18} and ω_{19}). This is fully supported by the fact that *N*-deuteration causes large shifts for all these modes. The salient point to note is that the frequencies of the symmetric (A_1) and asymmetric (B_2) vibrations of each mode are significantly different at all the investigated theoretical models. In particular the frequencies of the ω_{11} and ω_{12} modes are expected at 1404 and 1342 cm^{-1} (B3LYP) or 1409 and 1362 cm^{-1} (MP2). Therefore their values are not so close to give a single band at 1322 and 1319 cm^{-1} as assigned previously. The presence of a unique absorption could be caused instead by the low intensity predicted for the B_2 symmetry mode which, at least at the MP2 level, is expected negligible. Similarly, the down-shifts calculated upon *N*-deuteration are not fully consistent with the previous assignment of the spectrum of $BA(D_4)$ where the A_1 and B_2 δND frequencies were identified with the weak doublet at 1025–1022 cm^{-1} [5]. The theoretical spectra of BA and $BA(D_4)$ suggest thus a different assignment of the following bands: the couple of CN (1220 and 1019 cm^{-1}) and CC (919 and 914 cm^{-1}) stretching modes have frequencies in excellent agreement the observed values at 1222, 1010 and 939, 913 cm^{-1}, respectively, whereas the corresponding modes in $BA(D_4)$, 1041, 898 and 818, 757 cm^{-1}, well reproduce the absorption measured at 1025, 905 and 811, 768 cm^{-1}. The B3LYP frequencies of the CH_2 and CD_2 scissoring and wagging modes, nearly

Table 4
B3LYP/6-311++G(d,p) and Ar matrix frequencies of BA, 1,3,5,5′-tetradeuterobarbituric, BA(D_4), and 1,3-dideuterobarbituric, BA(D_2), acids

		B3LYP			Ar matrix		
		BA[a]	BA(D_4)	BA(D_2)	BA[b]	BA(D_4)[b]	BA(D_2)[c]
ω_1	νNH	3591 (49)	2634	2634	3437 (s)	2558 (m)	
ω_2	νNH	3589 (111)	2629	2629	3431 (sh)	2552 (w)	
ω_5	3νC=O sym	1820 (78)	1820	1820	1764 (s)	1757 (s)	1755 (s)
ω_6	3νC=O asym	1800 (892)	1780	1780	1754 (vs)	1734 (vs)	1733 (vs)
ω_7	νC4=O + νC6=O	1784 (604)	1778	1776	1747 (vs)	1730 (vs)	1728 (vs)
ω_8	δNH + νCN + δCH_2	1452 (49)	1223	1226	1433 (m)	1211 (m)	1210 (m)
ω_{10}	δNH + νCN + δCH_2	1416 (176)	1265	1263	1418 (s)	1269 (s)	1268 (s)
ω_{11}	νCN	1404 (136)	1398	1398		1408 (vs)	1404 1398 (vs)
ω_{12}	νCN	1342 (373)	1386	1379	1322 1319 (s)	1380 (vs)	1378 (vs)
ω_{14}	νCN + δNH	1220 (141)	1041	1102	1222 (vs)	1025 1022 (w)	1025 (w)
ω_{16}	νCN + δNH	1019 (11)	898	830	1010 (m)	905 (vw)	820 (w)
ω_{18}	νCC + νCN	919 (2)	818	913	939 (w)	811 (m)	
ω_{19}	νCC + νCN	914 (0)	757	851	913 (vw)	768 (w)	870 (m)
ω_{20}	γC2=O	752 (55)	750	750	754 (ms)	753 (s)	753 (s)
ω_{21}	γNH	687 (174)	517	537	674 670 (s)	511 508 (ms)	510 (m)
ω_{22}	γNH	681 (0)	458	462			
ω_{23}	δ ring	631 (1)	627	630	634 (vw)	632 (vw)	
ω_{24}	δC=O	623 (9)	570	591	619 (m)		
ω_{25}	γC4=O + γC6=O	588 (0)	598	645			
ω_{26}	δ ring	488 (14)	481	482	486 (mw)	480 (w)	
ω_{27}	δ ring	482 (41)	468	475	464 (m)	469 (w)	
ω_{28}	γC4=O + γC6=O	477 (>0)	396	442			
ω_9	δCH_2	1417 (18)	1043	1428	1498 (w)	1090 (vw)	1505 (vw)
ω_{13}	CH_2 wagging	1310 (8)	1174	1318	1353 1350 (s)	1167 (w)	1346 (m)
ω_{15}	CH_2 twisting	1219 (2)	941	1219	1192 (w)	955 (vw)	1195 (m)
ω_{17}	CH_2 rocking	953 (9)	887	953		878 (m)	

[a] IR intensities are given in parentheses (km mol^{-1}).
[b] Ref. [5].
[c] This study.

coincident with the MP2 values, reproduce the observed values with scaling factors 0.95–0.96. The frequencies of the twisting and rocking vibrations of the CH_2 (1219 and 953 cm^{-1}) and CD_2 (941 and 887 cm^{-1}) groups are in better agreement with the bands measured at 1192 cm^{-1} (CH_2) or 955 and 878 cm^{-1} (CD_2) in comparison with the previous assignment where they were identified with the absorptions at 1307 cm^{-1} (CH_2 twisting) and 905 cm^{-1} (CD_2 twisting) and 811 cm^{-1} (CD_2 rocking). Finally, the previous assignment can be substantially confirmed in the low-frequency zone where the in-plane and out-of-plane bending modes are well reproduced by the B3LYP and MP2 methods. The unique exception concerns the γC=O modes which, predicted well separated each other (752, 588 and 477 cm^{-1}), are not fully consistent with the previous assignment (768, 754 and 619 cm^{-1}). The new assignment is reported in Table 4.

The comparison between BA and TBA is a useful guide in the assignment of the observed spectra of TBA (Fig. 7). As suggested by ab initio and DFT results, the frequencies of some vibrational modes of TBA are indeed very close to those of BA thus their identification on the experimental

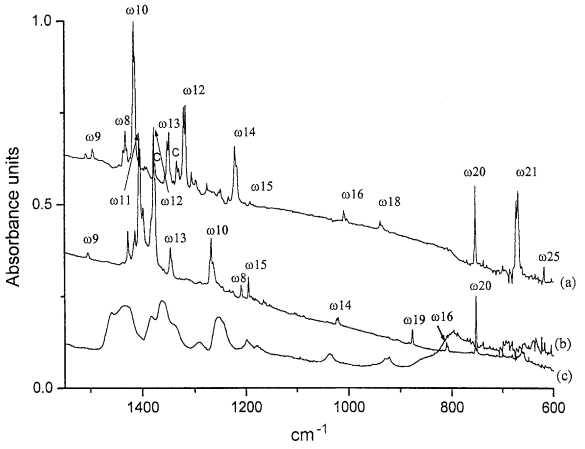

Fig. 6. FT-IR spectra of BA (a) and BAD_2 (b) in dilute Ar matrix and FT-IR spectrum of solid film of pure BA (c). Band combinations are marked by C.

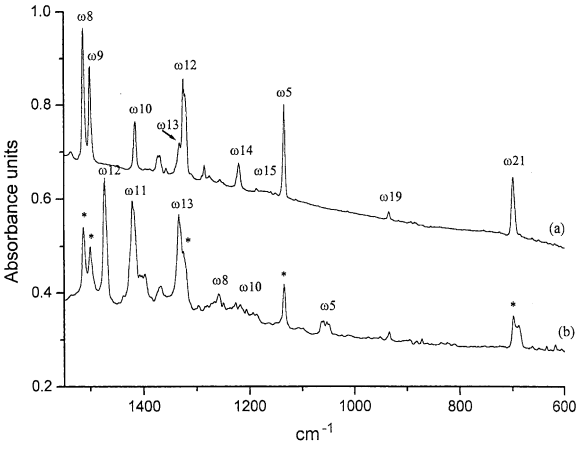

Fig. 7. FT-IR spectra of TBA (a) and $TBAD_2$ (b) in Ar matrix. Stars indicate bands of residual BA.

spectrum is quite easy (see Table 5). This is the case of the NH stretching (3415 cm^{-1}), C=O stretching (1750 and 1740 cm^{-1}) modes, some CN (1330 and 1220 cm^{-1}) and CC (934 cm^{-1}) stretching vibrations as well as the CH_2 normal modes which give absorptions at 1501 cm^{-1} (scissoring) and 1190 cm^{-1} (twisting). On the contrary, those modes localised on the C2=O group either disappear, the out-of-plane vibration, ω_{20}, or are found at lower frequency, as for the νC=S mode which is identified with the intense band at 1145 cm^{-1}. As a matter of fact the C=S stretching is remarkably mixed with some νCN as well as δNH modes. This fact explains the appreciable red-shift

Table 5
B3LYP/6-311++G(d,p) and Ar matrix frequencies of TBA and 1,3-dideuterobarbituric, $TBA(D_2)$, acids

		B3LYP		Ar matrix	
		TBA	$TBA(D_2)$	TBA	$TBA(D_2)$
ω_1	νNH	3587 (31)	2633 (27)		
ω_2	νNH	3583 (110)	2625 (68)	3415 (vs)	2533 (s)
ω_5	νC=S	1146 (199)	1058 (83)	1145 (vs)	1062–1049 (s)
ω_6	νC=O	1805 (378)	1799 (332)	1750 (vs)	1760 (vs)
ω_7	νC=O	1783 (656)	1777 (630)	1740 (vs)	1739 (vs)
ω_8	δNH + νCN + δCH_2	1542 (530)	1295 (89)	1513 (vs)	1269 (w)
ω_{10}	δNH + νCN + δCH_2	1425 (182)	1242 (99)	1416 (s)	1225 (w)
ω_{11}	νCN	1381 (46)	1401 (241)		1424 (vs)
ω_{12}	νCN	1334 (588)	1443 (756)	1330 (vs)	1481 (vs)
ω_{14}	νCN + δNH	1225 (102)	1092 (1)	1220 (m)	
ω_{16}	νCN + δNH	1024 (>0)	912 (7)		
ω_{18}	νCC + νCN	885 (2)	834 (23)		899 (w)
ω_{19}	νCC + νCN	898 (3)	848 (3)	934 (m)	876 (w)
ω_{21}	γNH	708 (159)	544 (73)	699 (s)	
ω_{22}	γNH	688 (>0)	472 (0)		
ω_9	δCH_2	1423 (4)	1414 (405)	1501 (s)	1505 (s)
ω_{13}	CH_2 wagging	1312 (9)	1315 (6)	1335 (m)	1342 (s)
ω_{15}	CH_2 twisting	1217 (>0)	1217 (>0)	1190 (vw)	
ω_{17}	CH_2 rocking	951 (10)	950 (14)		

predicted (88 cm^{-1}) for such vibration upon *N*-deuteration and the appearance of some bands at 1062 and 1049 cm^{-1}. As the theoretical frequencies indicate, another important difference in the TBA spectrum is the presence of intense bands in the region about 1500 cm^{-1} where instead BA shows only the weak CH_2 scissoring. The ω_8 and ω_{10} modes where dominant is the NH in plane bending vibration, were predicted at 1542 and 1425 cm^{-1} and were identified with the intense bands at 1513 and 1416 cm^{-1}, respectively. The assignment is supported by the spectrum of *N*,*N*′-dideuterobarbituric which is expected to exhibit such modes at 1295 and 1242 cm^{-1} in agreement with the bands observed at 1269 and 1225 cm^{-1}. As for BA, also for TBA the absorption relative to the B_2 *v*CN mode, ω_{11}, is predicted quite weak and therefore it could be absent in the measured spectrum. On the contrary its intensity noticeably increases upon *N*-deuteration and this explains the occurrence of the strong band observed at 1424 cm^{-1} and predicted at 1401 cm^{-1}. Another point consistent with our theoretical results is the small increase of the frequency of the NH out-of-plane bending in TBA (699 cm^{-1}) with respect to BA (674 cm^{-1}).

4.2.2. Concentrated matrix IR spectra

The FT-IR spectra of BA and TBA were measured in argon and nitrogen matrices at different concentrations and after cyclic annealing. The spectral perturbations observed at high concentration are similar to those measured in Ar matrix for BA [5] and have been already interpreted in terms of formation of closed rather than open structure dimers. Fig. 6 shows also the FT-IR spectrum of a solid film of pure BA. Self-association of BA in matrix is quickly witnessed by the broad absorptions at 3230 cm^{-1} (BA), 2350 cm^{-1} (BAD_2), and confirmed by the bands in the same region (3210 cm^{-1}) measured in solid film. Similarly, the appearance of broad absorptions at about 860–830 cm^{-1} (high concentrated matrix) or 800 cm^{-1} (solid film) in the spectral region typical of out-of-plane modes of hydrogen bonded NH groups further reveals the occurrence of self-aggregation.

A detailed study of the C=O stretching region of BA is quite complex because the presence of additional bands due to combinations (1772 cm^{-1}). However the unique significant change observed in the matrix spectrum by increasing concentration is the appearance of a broad band at 1734 cm^{-1}. This is fully consistent with the frequencies predicted for the three dimers here considered where the unique C=O stretching mode indeed sensitive to hydrogen bonding is the lowest frequency one. On the contrary, the BA film exhibits three broad absorptions, 1749, 1726 and about 1700 cm^{-1} in linea with the theoretical results on the BA trimer and hexamer where all the C=O and NH groups are hydrogen bonded and thus all the C=O stretching frequencies are different from those of the monomer.

In TBA spectrum evidence for a C=O···HN interaction is found in a weak absorption at 1708 cm^{-1}; the lack of additional bands in the zone of the C=S stretching is a convincing proof that dimerisation of TBA occurs only through C=O···HN hydrogen bonding. Moreover, the examination of the NH stretching zone of TBA shows only weak absorptions at 3210 cm^{-1} suggesting a lesser tendency to dimerisation in comparison with BA.

High concentration matrix spectra of BA show some additional bands at 1445, 1360 and 1233 cm^{-1} and a very weak absorption at 1030 cm^{-1} in the zone typical of the δNH modes and ring stretching vibrations. In addition, the previous Ar matrix spectrum [5] showed also a broad band at 1459 cm^{-1}. The presence of bands at higher frequency (1459 and 1445 cm^{-1}) with respect to the ω_8 and ω_{10} modes of the monomer is indicative of the formation of C2=O···HN as well as C4=O···HN hydrogen bonding interactions. B3LYP results suggest in fact that the ω_8 and ω_{10} modes of all BA dimers here considered experiment very similar blue-shifts. Also the appearance of absorptions at higher frequency (1360, 1233 and 1030 cm^{-1}) with respect to the ω_{12} (1322 cm^{-1}), ω_{14} (1222 cm^{-1}) and ω_{16} (1010 cm^{-1}) monomer bands suggest the occurrence of both C2=O···HN and C4=O···HN interactions. The B3LYP vibrational frequencies of the three BA dimers shown in Table 3 indicate that the exclusive formation of one hydrogen bond should be manifested in an exclusive blue-shift of the ω_{12} and ω_{14} (**2a** structure) or ω_{11} and ω_{16} (**2b** structure) frequency

modes. The matrix spectra of BA combined with the theoretical spectra of the dimeric structures provide evidences that BA dimerisation might involve C2═O···HN as well as C4═O···HN. It means that BA dimerisation might proceed through the **2c** structure or might cause the simultaneous formation of **2a**, **2b** and **2c** structures. The latter solution, already proposed to explain self-association of uracil in matrix [7], is fully supported by the fact that the BA dimers show stability indeed very close.

As for νC═O modes, also the previous region of the FT-IR solid film spectrum reveals that aggregation in condensed phase involves more than one C═O group and more than one NH group. Some bands (ω_{12}, ω_{14} and ω_{16}) move in fact at higher frequencies (1384, 1251 and 1038 cm^{-1}) with respect to dimer in agreement with our predictions on the BA hexamer and trimer. Surprisingly the ω_8 and ω_{10} modes (1460 and 1434 cm^{-1}) observed in solid film do not move too much from the corresponding modes of BA dimers measured at high concentration. This is not fully consistent with the hypothesis of the hexameric or trimeric structures here proposed for the condensed phase since the relative ω_8 and ω_{10} modes should be found at higher frequencies with respect to dimer, as already found for other normal modes. However, we cannot exclude that the dynamic process of molecular aggregation to form the solid film could lead to the formation of oligomers where some interaction sites are not yet involved in hydrogen bonding as occurs in the crystal. For example, cyclic dimers could interact with a third molecule through a single C═O···HN hydrogen bonding to form a trimer different from that here considered. Such structures could be intermediate steps towards the final crystal and we cannot exclude their presence in a solid film produced by condensing vapours at low temperatures.

5. Conclusions

1. BA and TBA consist of a single tautomeric species, trioxo and dioxo forms, respectively.
2. Substitution of oxygen with sulphur produces structural changes onto the ring framework caused by a variation of the π-conjugation in the CN bonds.
3. Cooperativity plays a negligible role in cyclic dimerisation processes and this is a consequence of the nearly equivalence of the C═O···HN hydrogen bonding interactions which BA may form.
4. Polar canonical forms –(C–O^-)═NH^+ are important in describing hydrogen bonded molecules since they reinforce the intermolecular interactions.
5. Thiobarbituric self-associates in matrix through C═O···HN interactions whereas aggregation of BA involves all the C═O and NH groups. It means that dimerisation of BA might proceed through the simultaneous formation of different dimeric structures which coexist in a low-temperature matrix.

References

[1] R. Ahuja, P. Caruso, D. Möbius, W. Paulus, H. Ringsdorf, G. Wildburg, Angew. Chem. Int. Ed. Engl. 32 (1993) 1033.
[2] T.M. Bohanon, S. Denzinger, R. Fink, W. Paulus, H. Ringsdorf, M. Weck, Angew. Chem. Int. Ed. Engl. 34 (1995) 58.
[3] T. Hasegawa, Y. Hatada, J. Nishio, J. Umemura, Q. Huo, R.M. Leblanc, J. Phys. Chem. B 103 (1999) 7505.
[4] A. Laschewsky, E. Wischerhoff, S. Denzinger, H. Ringsdorf, A. Delcorte, P. Bertrand, Chem. Euro. J. 3 (1997) 34.
[5] J. Barnes, L. Le Gall, J. Lauransan, J. Mol. Struct. 56 (1979) 15.
[6] P. Hobza, J. Sponer, Chem. Rev. 99 (1999) 3247.
[7] L. Bencivenni, F. Ramondo, A. Pieretti, N. Sanna, J. Chem. Soc., Perkin Trans. 2 (2000) 1685.
[8] J.E. Del Bene, W.B. Person, K. Szczepaniak, J. Phys. Chem. 99 (1995) 10705.
[9] J. Gu, J. Leszczynski, J. Phys. Chem. A 103 (1999) 577.
[10] J. Gu, J. Leszczynski, J. Phys. Chem. A 104 (2000) 7353.
[11] J. Barnes, M.A. Stuckey, W.J. Orville-Thomas, L. Le Gall, J. Lauransan, J. Mol. Struct. 56 (1979) 1.
[12] M.J. Frisch, G.W. Trucks, H.B. Schlegel, G.E. Scuseria, M.A. Robb, J.R. Cheeseman, V.G. Zakrzewski, J.A. Montgomery Jr., R.E. Stratmann, J.C. Burant, S. Dapprich, J.M. Millam, A.D. Daniels, K.N. Kudin, M.C. Strain, O. Farkas, J. Tomasi, V. Barone, M. Cossi, R. Cammi, B. Mennucci, C. Pomelli, C. Adamo, S. Clifford, J. Ochterski, G.A. Petersson, P.Y. Ayala, Q. Cui, K. Morokuma, D.K. Malick, A.D. Rabuck, K. Raghavachari, J.B. Foresman, J. Cioslowski, J.V. Ortiz, B.B. Stefanov, G. Liu, A. Liashenko, P. Piskorz, I. Komaroni, R. Gomperts, R.L. Martin, D.J. Fox, T. Keith, M.A. Al-Laham, C.Y. Peng,

A. Nanayakkara, C. Gonzalez, M. Challacombe, P.M.W. Gill, B. Johnson, W. Chen, M.W. Wong, J.L. Andres, C. Gonzalez, M. Head-Gordon, E.S. Replogle, J.A. Pople, GAUSSIAN98, Revision A.6; Gaussian Inc.: Pittsburgh, Pennsylvania, 1998.
[13] A.D. Becke, J. Chem. Phys. 98 (1993) 5648.
[14] C. Lee, W. Yang, R. Parr, Phys. Rev. B 37 (1988) 785.
[15] R. Poirer, R. Kari, I.G. Csizmadia, Handbook of Gaussian Basis Sets, Elsevier, Amsterdam, 1985.
[16] L.A. Curtiss, K. Raghavachari, J.A. Pople, J. Chem. Phys. 98 (1993) 1293.
[17] R.F.W. Bader, Atoms in Molecules: A Quantum Theory, Clarendon, Oxford, 1990.
[18] S. Dapprich, I. Komaromi, K. Suzie Byun, K. Morokuma, M.J. Frisch, J. Mol. Struct. (Theochem) 461–462 (1999) 1.
[19] S. Millefiori, A. Millefiori, J. Heterocycl. Chem. 26 (1989) 639.
[20] T.V. Soldatova, G.Ya. Kabo, A.A. Kozyro, M.L. Frenkel, Russ. J. Phys. Chem. 64 (1990) 177.
[21] B. Brunetti, V. Piacente, J. Chem. Eng. Data 44 (1999) 809.
[22] W. Bolton, Acta Crystallogr. 16 (1963) 166.
[23] B.V. Prasad, P. Uppal, P.S. Bassi, Chem. Phys. Lett. 276 (1997) 31.
[24] G.A. Jeffrey, An Introduction to Hydrogen Bonding, Oxford University Press, New York, 1997.